Journal of Mines, Metals and Fuels, *73(8): 2625-2637; 2025. DOI: 10.18311/jmmf/2025/49212*

Print ISSN : 0022-2755

Journal of Mines, Metals and Fuels

Contents available at: *www.informaticsjournals.co.in/index.php/jmmf*

Transient MHD Free Convection Flow over an Inclined Heated Plate: Analyzing Thermo-Diffusion and Diffusion-Thermo Effects in a Porous Medium

B. Nagaraju[1]*, P. Aparna[2], D. Madhavilatha[3], J. Venkata Madhu[4], M. Sravani[5], S. M. Bhati[6], G. Murali[7]

[1]*Palamuru University, Mahbubnagar - 509001, Telanagana, India; bnag2014@gmail.com*
[2]*VNR Vignana Jyoti Institute of Engineeringa and Technology, Bachupally - 500090, Telangana, India*
[3]*Sreyas Institute of Engineering and Technology, Hyderabad - 500068, Telangana, India*
[4]*VNR Vignana Jyoti Institute of Engineeringa and Technology, Bachupally - 500090, Telangana, India*
[5]*Malla Reddy University, Hyderabad - 500100, Telangana, India*
[6]*KBT College of Engineering, Nashik - 422001, Maharashtra, India*
[7]*Geethanjali College of Engineering and Technology, Hyderabad - 501301, Telangana, India*

Abstract

This research investigates the influence of thermodiffusion (Soret effect) and diffusion-thermo (Dufour effect) on transient Magneto-Hydro-Dynamic (MHD) free convective flow adjacent to a heated, inclined plate within a porous medium. The analysis incorporates thermal radiation as a key heat transfer mechanism, accounting for time-dependent variations in both velocity and temperature distributions. The porous structure introduces hydraulic resistance, altering fluid motion and thermal transport properties, while the plate's inclination modifies buoyancy-driven convection patterns. The applied magnetic field further complicates the dynamics through Lorentz force interactions. By addressing the coupled Soret and Dufour effects—frequently overlooked in basic models—the study enhances understanding of multispecies heat and mass transfer. The governing nonlinear partial differential equations are solved numerically via the finite difference method.Graphical results demonstrate how critical parameters affect velocity, temperature, and concentration profiles. This computational framework elucidates the complex interdependencies among electromagnetic, thermal, and hydrodynamic phenomena in porous media flows.

Major Findings: *Soret and Dufour effects significantly influence MHD free convection near an inclined plate in a porous medium. Radiation, magnetic field, and inclination modify flow and heat transfer. Numerical results show complex velocity, temperature, and concentration profiles.*

Keywords: *Diffusion-Thermo, Magneto-Hydro-Dynamics, Porous Medium, Thermo-Diffusion, Thermal Radiation*

1.0 Introduction

Free convective Magneto-Hydro-Dynamic (MHD) flows are crucial in numerous industrial, geophysical, and astrophysical applications. The extensive literature on convective MHD flows encompasses diverse fields. Furthermore, biological systems exhibit analogous phenomena, such as blood flow in the circulatory system and airflow in the respiratory tract. A classic example

**Author for correspondence*

is uranium isotope separation via gaseous diffusion in nuclear power plants. The simultaneous occurrence of heat and mass transfer introduces complexities to the driving potentials. Conversely, temperature gradients can induce mass fluxes, a phenomenon known as the Soret or thermal diffusion effect. While generally smaller than the effects described by Fourier's and Fick's laws, and often neglected, these cross-effects are significant in certain contexts. For example, thermal diffusion is exploited in isotope separation, and the diffusion-thermo effect cannot be ignored in gas mixtures involving both light (hydrogen-helium) and medium-weight (nitrogen-air) molecules. Recent years have witnessed considerable advancements in the study of heat and mass transfer in MHD flows, driven by their increasing relevance in various technological applications. The intricate interplay between magnetic fields, fluid motion, heat, and mass transfer necessitate sophisticated modeling and analysis to fully understand and exploit the potential of these systems. Further research into these coupled phenomena promises to yield significant advancements across a broad spectrum of scientific and engineering disciplines.

Recent research has delved into the intricate relationship between chemical reactions, variable fluid viscosity, and MHD effects on convective heat and mass transfer processes. For instance, Seddeck *et al.* [1] analyzed Hiemenz flow in a Darcy-type porous medium, examining how thermal radiation and magnetic fields affect mixed convection dynamics while considering viscosity variations and chemical reactions. Zueco *et al.*[2] adopted a network simulation approach to assess chemical reaction effects on MHD heat and mass transfer in boundary layer flows around a horizontal cylinder embedded in a Darcy-Forchheimer porous matrix. Further contributions include the work of Gireesh Kumar *et al.*[3], who explored unsteady MHD free convection along an infinite vertical plate, incorporating constant suction, heat sinks, and mass transfer with chemical reactions. Ibrahim[4] expanded the scope by investigating transient hydromagnetic natural convection, emphasizing the combined influence of chemical reactions, radiation absorption, wall transpiration, and heat sources. These studies collectively enhance understanding of multiphysical interactions in convective systems under diverse conditions. The study of MHD nanofluid flows through porous media has gained immense significance due to its wide-ranging applications in energy systems, biomedical engineering, and industrial processes such as cooling technologies and chemical reactors. Recent research highlights the critical role of external magnetic fields, thermal diffusion (Soret effect), and concentration gradients (Dufour effect) in enhancing or suppressing heat and mass transfer rates[5-8]. The increasing demand for efficient thermal management in high-performance systems necessitates a deeper understanding of non-Newtonian fluids, such as Casson and Powell-Eyring nanofluids, which exhibit unique rheological behaviors under MHD effects[9-13]. Additionally, the presence of chemical reactions and porous media introduces complex interactions that influence flow stability and thermal efficiency[14-16]. Recent studies emphasize the importance of boundary conditions, including thermal/mass Biot numbers and convective heating, in determining heat transfer performance[17-23]. Furthermore, the combined effects of thermophoresis and Brownian motion in nanofluids significantly alter thermal conductivity, making them superior to conventional fluids in heat exchangers and electronic cooling systems[24-29]. The exploration of bio-convection in hybrid nanofluids, driven by motile microorganisms, has opened new avenues in bioengineering and drug delivery systems[30]. Despite extensive analytical and numerical investigations, gaps remain in understanding the coupled effects of radiation, Hall currents, and variable suction in unsteady flows[31-34]. Advanced computational techniques, such as finite element and finite difference methods, have been employed to solve these nonlinear problems, but experimental validation remains limited[35-39]. Moreover, the impact of magnetic dipoles and ferrofluids on convective heat transfer in porous enclosures presents novel challenges in optimizing energy systems[40]. Recent works also highlight the need for optimizing slip conditions and activation energy in stretching sheet flows, which are crucial in polymer processing and metallurgy[41-43]. Given these advancements, this study aims to consolidate existing knowledge while addressing unresolved questions related to multi-physical interactions in MHD nanofluid flows, providing a foundation for future innovations in thermal and mass transport applications[44-45]. The integration of machine learning and response surface methodologies (RSM) in fluid dynamics further underscores the potential for data-

driven optimization in industrial processes[46]. Thus, this research is motivated by the need to bridge theoretical, computational, and experimental gaps in MHD nanofluid flows, ensuring sustainable and efficient thermal systems for next-generation technologies. These investigations collectively contribute to a deeper understanding of the coupled phenomena governing hydromagnetic convective transport in porous media under diverse conditions.The present study was significantly shaped by prior research in references[47,48], which informed its methodology and theoretical framework.

The present analysis incorporates chemical reaction and thermal radiation absorption, motivated by the extensive potential for industrial applications and relevant prior research. Our objective is to expand upon existing literature by examining a more generalized problem encompassing joint effects of diffusion within transient Magnetohydrodynamic flow and heat transfer scenario over a porous plate. Further, the influence of various parameters is systematically analyzed. A finite difference method, chosen for its computational efficiency, provides the numerical solution to this complex problem.

2.0 Mathematical Formulation

This study examines a two-dimensional, time-dependent MHD free convective flow of an electrically conducting, viscous, and incompressible fluid past a semi-infinite inclined porous plate. The system incorporates the effects of thermal radiation and chemical reactions. A Cartesian coordinate system is employed, with the X-axis aligned parallel to the plate and the Y-axis perpendicular to it. Due to the assumption of an infinitely extended plate, all physical properties remain invariant along the plate's length, simplifying the analysis of the flow dynamics. The investigation focuses on the interplay between magnetic fields, thermal radiation, and chemical reactivity in influencing fluid behavior. The inclined porous plate introduces additional complexity, as buoyancy-driven convection interacts with the applied magnetic field. By considering these factors, the study aims to provide insights into the combined effects of external forces and material properties on the flow characteristics of electrically conductive fluids.

The following are the flow governing equations

Momentum Equation:

$$\frac{\partial u'}{\partial t'} = g\beta(T' - T'_\infty)(\cos\alpha) + g\beta^*(C' - C'_\infty)(\cos\alpha)$$

$$+\nu\frac{\partial^2 u'}{\partial y'^2} - \left(\frac{\sigma B_o^2}{\rho} + \frac{\nu}{K'}\right)u' \qquad (1)$$

Energy Equation:

$$\rho C_p\frac{\partial T'}{\partial t'} = \kappa\frac{\partial^2 T'}{\partial y'^2} - \frac{\partial q_r}{\partial y'} + \nu\left(\frac{\partial u'}{\partial y'}\right)^2 + Q'(T' - T'_\infty)$$

$$+Q'(T' - T'_\infty) \qquad (2)$$

Species Diffusion Equation:

$$\frac{\partial C'}{\partial t'} = D\frac{\partial^2 C'}{\partial y'^2} - K_r(C' - C'_\infty) + \frac{D_m k_T}{T_m}\frac{\partial^2 T'}{\partial y'^2} \qquad (3)$$

With the following initial and boundary conditions:

$$t' \le 0 : u' = 0,\ T' = T'_\infty,\ C' = C'_\infty \ \ for\ all\ \ y'$$

t'> 0 : u' =UO, T'= T'∞ + (T'w= T'∞) At', C'= C'∞ +(C'w= T'∞) At', at y' = 0, u' → 0, T'→ 0, C'→ 0, as y'→ ∞ (4)

The radiative heat flux

$$q_r = -\frac{4\sigma}{3\kappa}\frac{\partial^2 T'^4}{\partial y'} \qquad (5)$$

By using Taylor series, we get

$$T'^4 \cong 4T'^3_\infty T' - 3T'^4_\infty \qquad (6)$$

By using Equations (5) and (6), Equation (2) reduces to

$$\frac{\partial T'}{\partial t'} = \frac{\kappa}{\rho C_p}\frac{\partial^2 T'}{\partial y'^2} - \frac{16\sigma T'^3_\infty}{3k_1\rho C_p}\frac{\partial^2 T'}{\partial y'^2} \qquad (7)$$

Proposed dimensionless parameters in Equations (1)-(3) and (7):

$$y=\frac{y'U_o}{\nu},t=\frac{t'U_o}{\nu},u=\frac{u'}{U_o},\ \theta=\frac{T'-T'_\infty}{T'_w-T'_\infty},\ C=\frac{C'-C'_\infty}{C'_w-C'_\infty},$$

$$Gr=\frac{g\beta\nu(T'_w-T'_\infty)}{U_o^3},\ Sc=\frac{\nu}{D},\ Gc=\frac{g\beta^*\nu(C'_w-C'_\infty)}{U_o^3},$$

$$\Pr=\frac{\mu C_p}{\kappa},M=\left(\frac{\sigma B_o^2}{\rho}\right)\frac{\nu}{U_o^2},Ec=\frac{U_o^2}{C_p(T'_w-T'_\infty)},\ Q=\frac{\nu Q'}{\rho C_p U_o^2},$$

$$K=\frac{K'U_o^2}{\nu^2},N=\frac{\kappa U_o^2}{4\nu^2\sigma T'^3_\infty},\ k_r=\frac{K_r\nu}{U_o^2},$$

$$Du=\frac{D_m k_T(C'_w-C'_\infty)}{C_S C_P(T'_w-T'_\infty)},\ Sr=\frac{D_m k_T(T'_w-T'_\infty)}{\nu T_m(C'_w-C'_\infty)} \quad \Big| \tag{8}$$

In Equations (1), (2), (3) and (7) reduces to

$$\frac{\partial u}{\partial t}=\frac{\partial^2 u}{\partial y^2}-(M+\frac{1}{K})u+(Gr)(\cos\alpha)\theta+(Gc)(\cos\alpha)C \tag{9}$$

$$(\Pr)\frac{\partial\theta}{\partial t}=\left(1+\frac{4}{3N}\right)\frac{\partial^2\theta}{\partial y^2}+(\Pr)(Ec)\left(\frac{\partial u}{\partial y}\right)^2+$$

$$(Du)(\Pr)\left(\frac{\partial^2 C}{\partial y^2}\right)-(\Pr)(Q)\theta \tag{10}$$

$$\frac{\partial C}{\partial t}=\frac{1}{Sc}\frac{\partial^2 C}{\partial y^2}+Sr\left(\frac{\partial^2\theta}{\partial y^2}\right)-(k_r)C \tag{11}$$

The boundary conditions in non-dimensional form

$$\left.\begin{array}{l} t\le 0:\ u=0,\ \theta=0,\ C=0\ \ for\ \ all\ \ y \\ t>0:\begin{cases} u=1,\ \theta=t,\ C=t\ \ at\ \ y=0 \\ u\to 0,\ \theta\to 0,\ C\to 0\ \ as\ \ y\to\infty \end{cases}\end{array}\right\} \tag{12}$$

Engineering quantities are

$$\tau=\frac{\tau_w}{\rho u_w^2},\ \tau_w=\left[\mu\frac{\partial u}{\partial y}\right]_{y'=0}=\rho U_o^2 u'(0)=\left[\frac{\partial u}{\partial y}\right]_{y=0} \tag{13}$$

$$N_u(x')=-\left[\frac{x'}{(T'_w-T'_\infty)}\frac{\partial T'}{\partial y'}\right]_{y'=0}$$

$$\text{then}\ \ Nu=\frac{N_u(x')}{R_{e_x}}=-\left[\frac{\partial\theta}{\partial y}\right]_{y=0} \tag{14}$$

$$S_h(x')=-\left[\frac{x'}{(C'_w-C'_\infty)}\frac{\partial C'}{\partial y'}\right]_{y'=0}$$

$$\text{then}\ \ Sh=\frac{S_h(x')}{R_{e_x}}=-\left[\frac{\partial C}{\partial y}\right]_{y=0} \tag{15}$$

3.0 Methods

Numerical modeling and simulation are more efficient and cost-effective methods for solving complex mathematical equations than traditional methods. These models accurately represent the physical system under investigation, allowing for rigorous analysis and validation against real-world observations. The finite difference method, used in this study, is a versatile and powerful technique for addressing linear and nonlinear partial and ordinary differential equations. It is a valuable tool for future research in fields like physics and mechanical engineering, and its applicability extends to a broad range of complex systems, indicating continued progress in these fields.

We solved the system of equations using the finite difference method. The Equations (9), (10), and (11) will get the following form

$$\left(\frac{u_i^{j+1}-u_i^j}{\Delta t}\right)=\left(\frac{u_{i+1}^j-2u_i^j+u_{i-1}^j}{(\Delta y)^2}\right)-\left(M+\frac{1}{K}\right)u_i^j$$

$$+(G\ )(\cos\alpha)\theta_i^j+(G\ )(\cos\alpha)C_i^j \tag{16}$$

$$(\Pr)\left(\frac{\theta_i^{j+1}-\theta_i^j}{\Delta t}\right)=\left(1+\frac{4N}{3}\right)\left(\frac{\theta_{i+1}^j-2\theta_i^j+\theta_{i-1}^j}{(\Delta y)^2}\right)+$$

$$(\Pr)(Ec)\left(\frac{u_{i+1}^j-u_i^j}{\Delta y}\right)^2+(\Pr)(Du)\left(\frac{C_{i+1}^j-2C_i^j+C_{i-1}^j}{(\Delta y)^2}\right)$$

$$-(\Pr)(Q)\theta_i^j \tag{17}$$

$$(\delta)\left(\frac{C_i^{j+1}-C_i^j}{\Delta t}\right)=\left(\frac{C_{i+1}^j-2C_i^j+C_{i-1}^j}{(\Delta y)^2}\right)-(k_r)(\delta)C_i^j$$

$$+(\delta)(\delta)\left(\frac{\theta_{i+1}^j-2\theta_i^j+\theta_{i-1}^j}{(\Delta y)^2}\right) \quad (18)$$

$$\left.\begin{array}{l} t\le 0:\ u_i^j=0,\ \theta_i^j=0,\ C_i^j=0 \ \ for\ all\ y \\ t>0:\begin{cases} u_i^j=1,\ \theta_i^j=t,\ C_i^j=t \ \ at\ y=0 \\ u_i^j\to 0,\ \theta_i^j\to 0,\ C_i^j\to 0 \ \ as\ y\to\infty \end{cases} \end{array}\right\} \quad (19)$$

$$\frac{\partial u}{\partial t}=\frac{u_i^{j+1}-u_i^j}{\Delta t}+O(\Delta t),$$

$$\frac{\partial \theta}{\partial t}=\frac{\theta_i^{j+1}-\theta_i^j}{\Delta t}+O(\Delta t),$$

$$\frac{\partial C}{\partial t}=\frac{C_i^{j+1}-C_i^j}{\Delta t}+O(\Delta t),$$

$$\frac{\partial^2 u}{\partial y^2}=\frac{u_{i+1}^j-2u_i^j+u_{i-1}^j}{(\Delta y)^2}+O(\Delta y)^2,$$

$$\frac{\partial^2 \theta}{\partial y^2}=\frac{\theta_{i+1}^j-2\theta_i^j+\theta_{i-1}^j}{(\Delta y)^2}+O(\Delta y)^2 \ \&$$

$$\frac{\partial^2 C}{\partial y^2}=\frac{C_{i+1}^j-2C_i^j+C_{i-1}^j}{(\Delta y)^2}+O(\Delta y)^2$$

For the consistency of Equation (16), we estimate

$$\left\{\left(\frac{u_i^{j+1}-u_i^n}{\Delta t}\right)-\left(\frac{u_{i+1}^j-2u_i^j+u_{i-1}^j}{(\Delta y)^2}\right)+\left(M+\frac{1}{K}\right)u_i^j-\right.$$

$$\left.(Gr)(\cos\alpha)\theta_i^j-(Gc)(\cos\alpha)C_i^j\right\}$$

$$-\left\{\frac{\partial u}{\partial t}-\frac{\partial^2 u}{\partial y^2}+(M+\frac{1}{K})u-(Gr)(\cos\alpha)\theta-(Gc)(\cos\alpha)C\right\}_{i,j}$$

$$=O(\Delta t)+O(\Delta y)^2 \quad (20)$$

For consistency of Equation (17), we estimate

$$\left\{(\Pr)\left(\frac{\theta_i^{j+1}-\theta_i^j}{\Delta t}\right)-\left(1+\frac{4N}{3}\right)\left(\frac{\theta_{i+1}^j-2\theta_i^j+\theta_{i-1}^j}{(\Delta y)^2}\right)-\right.$$

$$(\Pr)(Ec)\left(\frac{u_{i+1}^j-u_i^j}{\Delta y}\right)^2-(\Pr)(Du)\left(\frac{C_{i+1}^j-2C_i^j+C_{i-1}^j}{(\Delta y)^2}\right)+($$

$$\left.(\Pr)(Q)\theta_i^j\right\}-\left\{(\Pr)\frac{\partial\theta}{\partial t}-\left(1+\frac{4}{3N}\right)\frac{\partial^2\theta}{\partial y^2}-(\Pr)(Ec)\left(\frac{\partial u}{\partial y}\right)^2\right.$$

$$\left.-(Du)(\Pr)\left(\frac{\partial^2 C}{\partial y^2}\right)+(\Pr)(Q)\theta\right\}_{i,j}=O(\Delta t)+O(\Delta y)^2 \quad (21)$$

Similarly, concerning Equation (18)

$$\left\{(Sc)\left(\frac{C_i^{j+1}-C_i^j}{\Delta t}\right)-\left(\frac{C_{i+1}^j-2C_i^j+C_{i-1}^j}{(\Delta y)^2}\right)+\right.$$

$$\left.(k_r)(Sc)C_i^j-(Sc)(Sr)\left(\frac{\theta_{i+1}^j-2\theta_i^j+\theta_{i-1}^j}{(\Delta y)^2}\right)\right\}$$

$$-\left\{(Sc)\frac{\partial C}{\partial t}-\frac{\partial^2 C}{\partial y^2}-(Sc)(Sr)\left(\frac{\partial^2\theta}{\partial y^2}\right)+(k_r)(Sc)C\right\}_{i,}$$

$$=O(\Delta t)+O(\Delta y)^2 \quad (22)$$

The Equations (20)-(22) are solved using (19), the system of equations are as follows

$$A_i X_i = B_i \ (i=1 \text{ to } n) \quad (23)$$

For velocity, temperature, and concentration, the Thomas Algorithm has solved the aforementioned system of equations. Various values of Δt are used in the calculations to demonstrate the convergence of the finite difference approach. Convergence and stability are hence features of the finite difference method.

4.0 Results and Discussion

The influence of key parameters on fluid dynamics and thermal behavior is analyzed through a series of

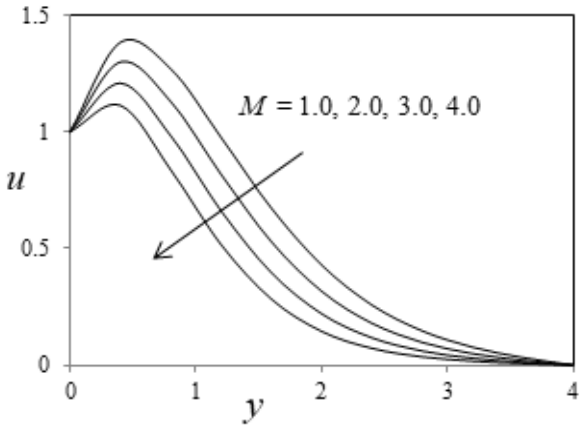


Figure 1. Velocity profiles for different values of Magnetic field.

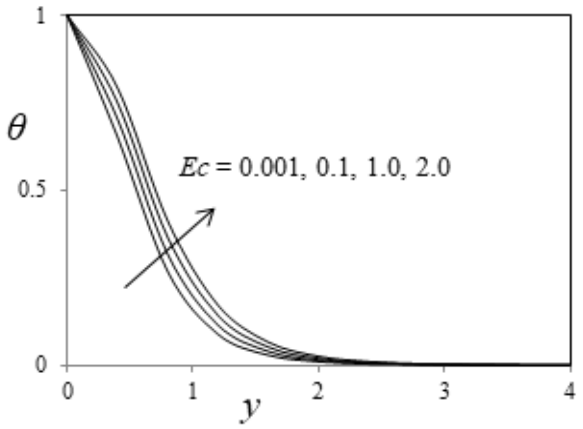


Figure 4. Temperature profiles for different values of Eckert number.

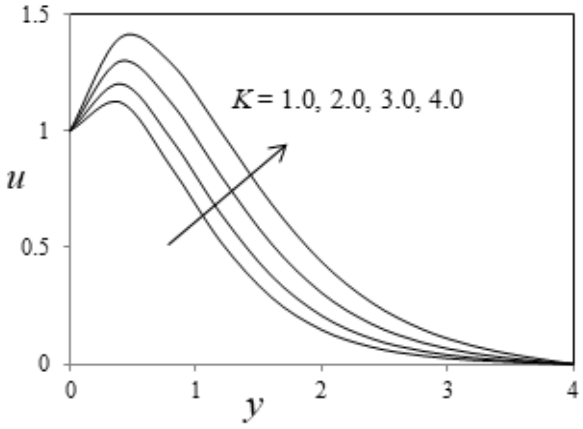


Figure 2. Velocity profiles for different values of Permeability parameter.

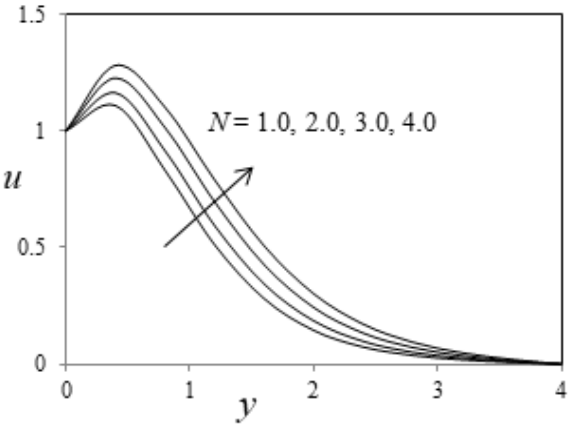


Figure 5. Velocity profiles for different values of Thermal radiation parameter.

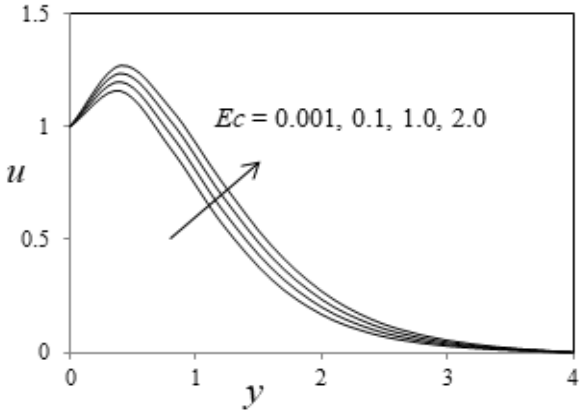


Figure 3. Velocity profiles for different values of Eckert number.

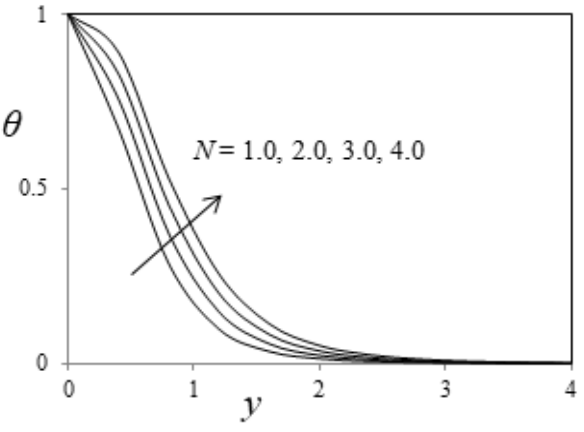


Figure 6. Temperature profiles for different values of Thermal radiation parameter.

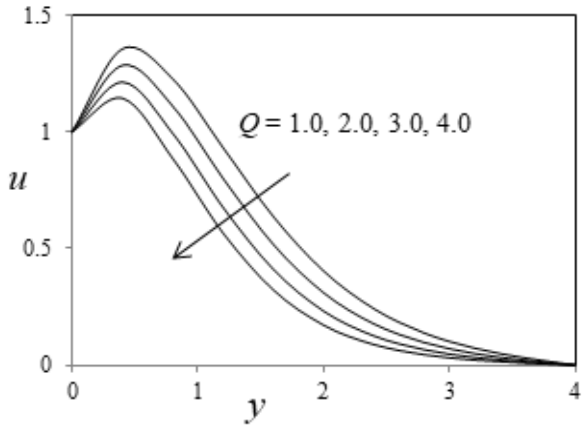


Figure 7. Velocity profiles for different values of Heat absorption parameter.

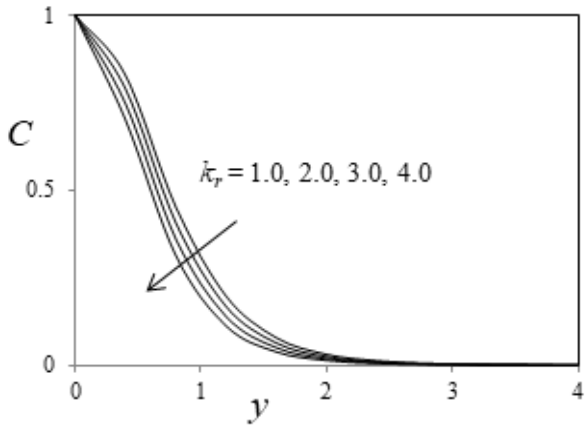


Figure 10. Concentration profiles for different values of Chemical reaction parameter.

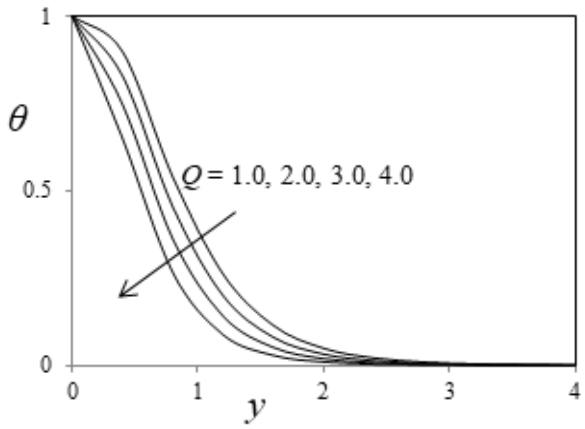


Figure 8. Temperature profiles for different values of Heat absorption parameter.

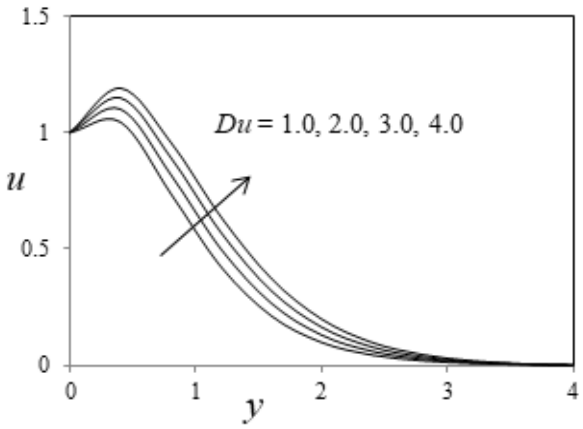


Figure 11. Velocity profiles for different values of Dufour number.

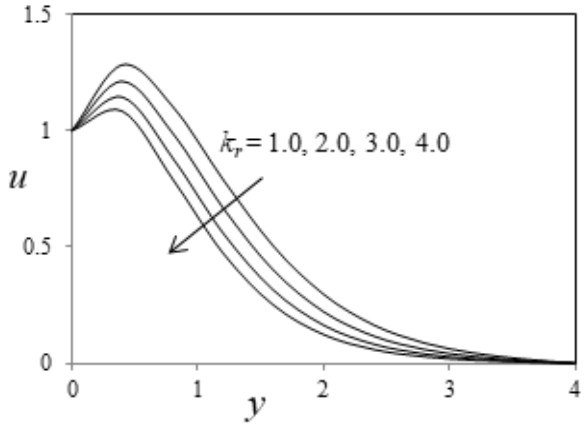


Figure 9. Velocity profiles for different values of Chemical reaction parameter.

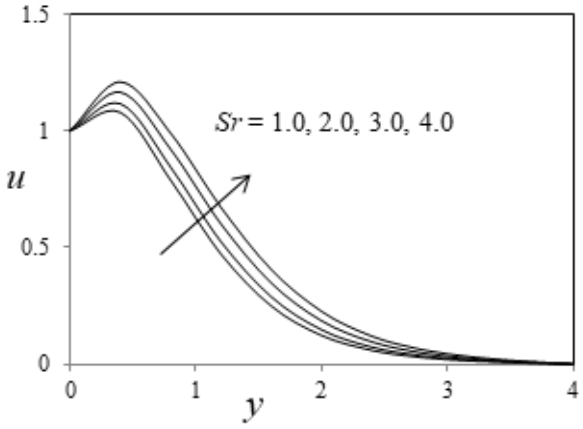


Figure 12. Velocity profiles for different values of Soret number.

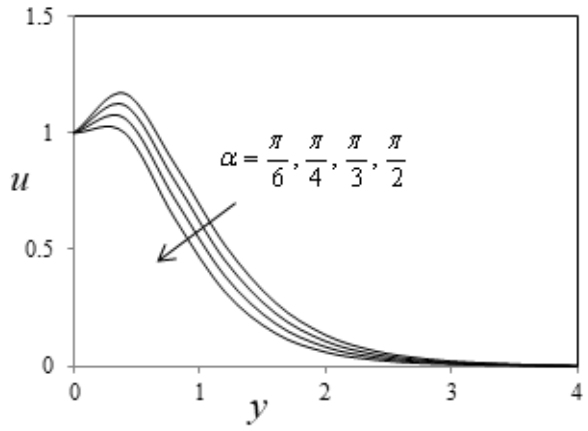


Figure 13. Velocity profiles for different values of Phase angle.

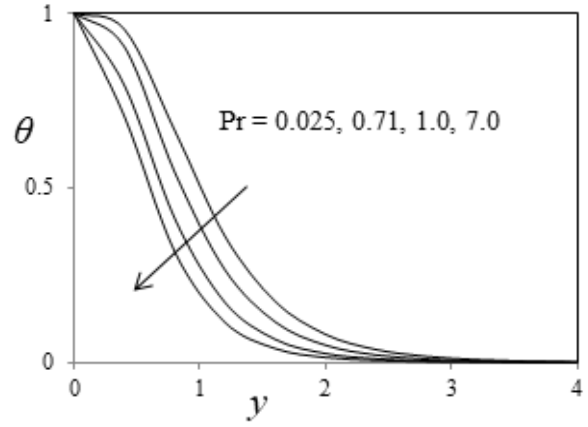


Figure 14. Temperature profiles for different values of Prandtl number.

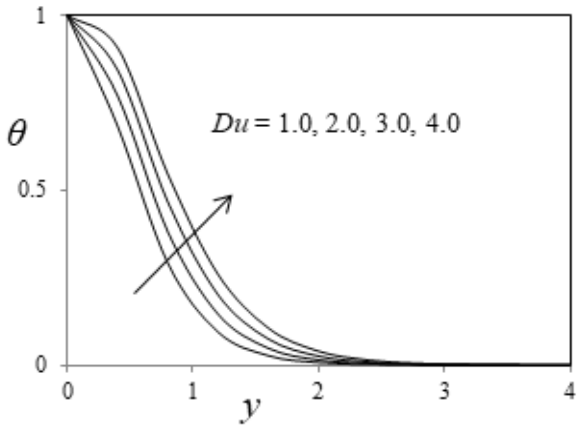


Figure 15. Temperature profiles for different values of Dufour number.

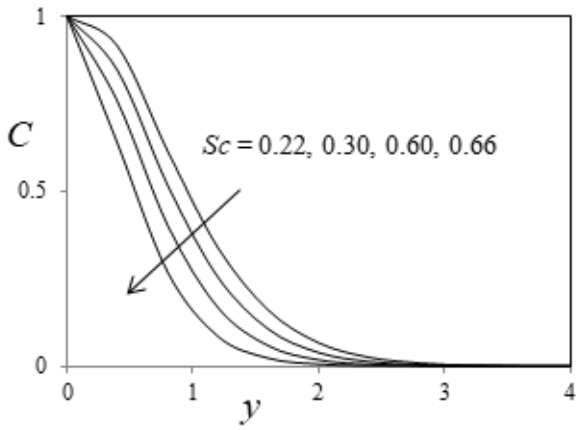


Figure 16. Concentration profiles for different values of Schmidt number.

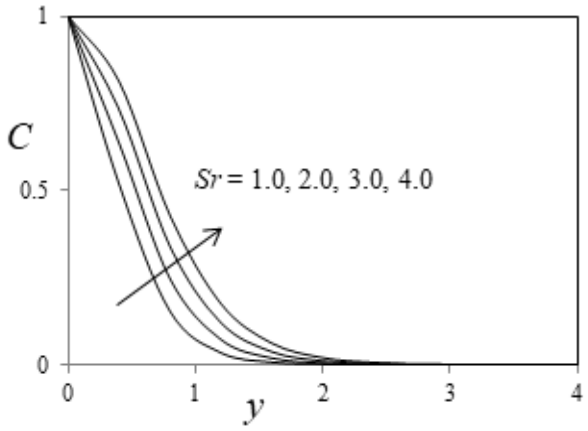


Figure 17. Concentration profiles for different values of Soret number.

figures. Figure 1 demonstrates how the Hartmann number, which depends on the strength of the applied magnetic field, affects fluid velocity. The Lorentz force, generated by the interaction between the magnetic field and the electrically conductive fluid, leads to a reduction in velocity. Conversely, Figure 2 reveals that higher permeability parameters enhance fluid velocity within the boundary layer, as the porous medium's reduced resistance facilitates greater fluid flow.

The role of viscous dissipation, represented by the Eckert number, is illustrated in Figures 3 and 4, where both temperature and velocity rise with increased dissipation. Additionally, the thermal radiation

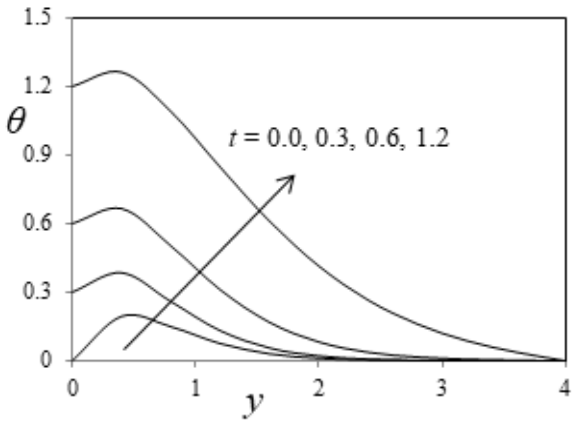


Figure 18. Temperature profiles for different values of time.

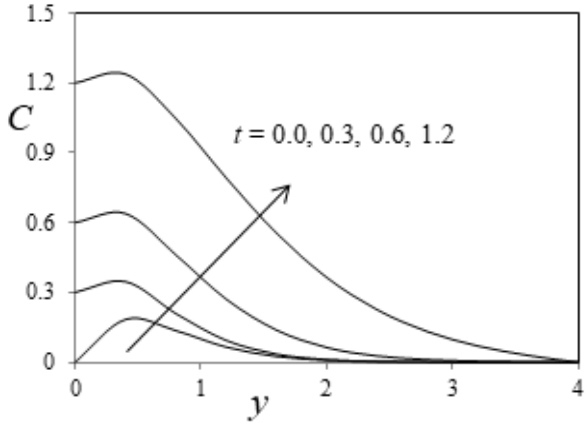


Figure 19. Concentration profiles for different values of time.

Table 1. Skin friction results (τ)

M	*K*	E_c	*N*	*Q*	*Sr*	*Du*	*Kr*	*α*	*t*	*τ*
1.0	1.0	0.0010	1.0	1.0	1.0	1.0	1.0	$\pi/2$	1.0	1.31654894
2.0	1.0	0.0010	1.0	1.0	1.0	1.0	1.0	$\pi/2$	1.0	1.27945621
1.0	2.0	0.0010	1.0	1.0	1.0	1.0	1.0	$\pi/2$	1.0	1.33025491
1.0	1.0	0.1000	1.0	1.0	1.0	1.0	1.0	$\pi/2$	1.0	1.33462159
1.0	1.0	0.0010	2.0	1.0	1.0	1.0	1.0	$\pi/2$	1.0	1.34116954
1.0	1.0	0.0010	1.0	2.0	1.0	1.0	1.0	$\pi/2$	1.0	1.29405618
1.0	1.0	0.0010	1.0	1.0	2.0	1.0	1.0	$\pi/2$	1.0	1.35026459
1.0	1.0	0.0010	1.0	1.0	1.0	2.0	1.0	$\pi/2$	1.0	1.35842165
1.0	1.0	0.0010	1.0	1.0	1.0	1.0	2.0	$\pi/2$	1.0	1.29026489
1.0	1.0	0.0010	1.0	1.0	1.0	1.0	1.0	$2\pi/3$	2.0	1.27036217

parameter significantly elevates fluid temperature, expanding the thermal boundary layer and boosting velocity, as depicted in Figures 5 and 6. Figures 7 and 8, with a fixed value of 1.0, explore the impact of the heat absorption coefficient on temperature and velocity profiles, further clarifying the interplay between thermal and hydrodynamic effects. By acting as a thermal sink and lowering fluid temperature and thermal buoyancy effects, heat absorption lowers fluid velocity. Figures 9 and 10 illustrate how the chemical reaction parameter affects the outcome. Figure 11 illustrates how the velocity distribution varies for various Dufour numbers in relation to a particular parameter. While velocity clearly increases as the Dufour number rises, Figure 12 shows that velocity also rises when the Soret number rises. Figure 13 shows how the phase angle affects the velocity field, with velocity decreasing as the phase angle increases. The relationship between the temperature field and the Prandtl number is seen in Figure 14, where a higher Prandtl number results in a lower temperature.

The effects of the Dufour number on fluid temperature are depicted in Figure 15, which shows that diffusion thermal effects have little impact on temperature. The fluid temperature rises in tandem with the Dufour number. The effect of the Schmidt number on the concentration field is depicted in Figure 16, which indicates that the fluid medium concentration in the boundary layer area dramatically drops as the Schmidt number rises. Figure 17 illustrates how the concentration field increases as the Soret number rises.

Figures 18 and 19 illustrate how time affects temperature and concentration profiles, demonstrating that as time values increase, so do temperature and concentration. Table 1 presents skin-friction profiles influenced by flow parameters. Table 2 shows Nusselt number variations affected by Prandtl, Eckert, time, Dufour, and heat absorption. Table 3 lists Sherwood number profiles dependent on time, chemical reaction, Schmidt number, and Soret effects.

Table 2. Rate of heat transfer (Nu) values

Pr	*Ec*	*N*	*Q*	*Du*	*t*	*Nu*
0.71	0.001	1.0	1.0	1.0	1.0	0.68741184
7.00	0.001	1.0	1.0	1.0	1.0	0.55413624
0.71	0.100	1.0	1.0	1.0	1.0	0.72594875
0.71	0.001	2.0	1.0	1.0	1.0	0.71439985
0.71	0.001	1.0	2.0	1.0	1.0	0.60573605
0.71	0.001	1.0	1.0	2.0	1.0	0.70150548
0.71	0.001	1.0	1.0	1.0	2.0	0.72158491

Table 3. Rate of mass transfer (Sh) values

Sc	*Kr*	*Sr*	*t*	*Sh*
0.22	1.0	1.0	1.0	1.42916652
0.30	1.0	1.0	1.0	1.32480057
0.22	2.0	1.0	1.0	1.36820629
0.22	1.0	2.0	1.0	1.44571133
0.22	1.0	1.0	2.0	1.45026987

5.0 Conclusions

This study investigates the coupled thermo-diffusion and diffusion-thermo effects within unsteady Magneto-Hydro-Dynamic (MHD) free convection flow adjacent to a heated, inclined plate embedded in a porous medium. The analysis delves into the intricate interplay between thermal and mass diffusion processes under the influence of an applied magnetic field, considering the transient nature of the flow. The inclined orientation of the heated plate introduces an additional geometric complexity, impacting the buoyancy-driven flow patterns. The porous medium further modifies the fluid dynamics, introducing resistance to flow and altering heat and mass transfer characteristics. The research aims to provide a comprehensive understanding of the combined influence of these factors on the flow field, temperature distribution, and concentration profiles. The investigation likely employs numerical or analytical techniques to solve the governing equations, which incorporate the relevant conservation laws for mass, momentum, energy, and species concentration, accounting for the effects of MHD, buoyancy forces, and the porous medium's permeability.

- The results will contribute to a more refined understanding of coupled transport processes in complex systems.
- Concentration profiles show a positive correlation with time and Soret number, while a negative correlation with Schmidt number and chemical reaction parameter.
- These findings provide a comprehensive understanding of the interplay between these parameters and the resulting flow characteristics.
- This understanding is crucial for applications involving porous media transport phenomena under the influence of magnetic fields, such as those encountered in geothermal energy extraction, filtration processes, and certain types of material processing.

6.0 References

1. Seddeek MA, Darwish AA, Abdelmeguid MS. Effects of chemical reaction and variable viscosity on hydromagnetic mixed convection heat and mass transfer for Hiemenz flow through porous media with radiation. Communications in Nonlinear Science and Numerical Simulation. 2007; 12(2):195-213. https://doi.org/10.1016/j.cnsns.2006.02.008
2. Zueco J, Beg OA, Tasveer A, Takhar HS. Numerical study of chemically reactive buoyancy-driven heat and mass transfer across a horizontal cylinder in a non-Darcian porous regime. J Porous Media. 2008 https://doi.org/10.1615/JPorMedia.v12.i6.30
3. Gireesh Kumar J, Satyanarayana PV, Ramakrishna S. Effects of chemical reaction and mass transfer on MHD unsteady free convection flow past an infinite vertical plate with constant suction and heat sink, Journal of Ultra Scientist. 2009; 21(3):12-28.
4 Ibrahim FS, Elaiw AM, Bakr AA. Effect of the chemical reaction and radiation absorption on the unsteady MHD free convection flow past a semi-infinite vertical permeable moving plate with heat source and suction. Communications Nonlinear Science Numerical Simulation. 2008; 13:1056-1066. https://doi.org/10.1016/j.cnsns.2006.09.007
5. Gundagani M, Javvaji V, Gadipalli D, Pallerla S, Al-Mdallal Q, Bhati S. A numerical study on mhd 3-d casson-nanofluid flow past an exponentially stretching sheet with double cattaneo-christov diffusion effects. Rev Int. Métodos Numér. Cálc. Diseño Ing. 2025; 41(2):21. https://www.scipedia.com/public/Gundagani_et_al_2025a
6. Deepa G, Gundagani M. Analysis of Soret and Dufour effects on unsteady MHD flow past a semi-infinite vertical porous plate via finite difference method. Int J Appl Phys Math. 2014; 4(5):332-344. https://doi.org/10.7763/IJAPM.2014.V4.306
7. Kirubaharan DR, Subhashini AD, Murali G. Study of three-dimensional casson-nanofluid flow due to a linear porous stretching sheet in the presence of double diffusion effects. Adv Syst Sci Appl. 2024; 24(3):90-103. https://doi.org/10.25728/assa.2024.2024.03.1539
8. Vanaja GG, Srinivas B, Suresh Babu B, Goud S, Hendy AS, Ali MR, Ali MM. Influence of variable viscosity and slip on heat and mass transfer of immiscible fluids in a vertical channel. Case Studies in Thermal Engineering. 2024:104368 https://doi.org/10.1016/j.csite.2024.104368
9. Gul T, Nasir S, Berrouk AS, Raizah Z, Alghamdi W, Ali I, Bariq A. Simulation of the water-based hybrid nanofluids flow through a porous cavity for the applications of the heat transfer. Scientific Reports. 2023; 13(1):7009. https://doi.org/10.1038/s41598-023-33650-w
10. Murali G, Deepa G, Madhu JV, Kasturi VN, Bhati SM, Babu NN. Three dimensional chemically reacting oldroyd-B fluid + nanofluid flow in presence of thermophoresis and Brownian motion effects.

Discontinuity, Nonlinearity, and Complexity. 2025; 14(2):373-388. https://doi.org/10.5890/DNC.2025.06.010

11. Boujelbene M, Rehman S, Jazaa Y, Hashim, Dhaou MH. Thermodynamics of hydromagnetic boundary layer flow of Prandtl nanofluid past a heated stretching cylindrical surface with interface slip. Journal of the Taiwan Institute of Chemical Engineers. 2024; 155:105310. http://dx.doi.org/10.1016/j.jtice.2023.105310
12. Lone SA, Raizah Z, Saeed A, Bognár G. Statistical computation for heat and mass transfers of water-based nanofluids containing Cu, Al_2O_3, and TiO_2 nanoparticles over a curved surface. Scientific Reports. 2024; 14(1):6908. http://dx.doi.org/10.1038/s41598-024-57532-x
13. Bhati SM, Murali G, Sanjay CH. Law of electric fields via Bianchi identities. J Appl Sci Eng. 2022; 25(4):759-762. https://doi.org/10.6180/jase.202208_25(4).0011
14. Nagasmitha BR, Nagendramma V, Ahmed N, Marutamanikandan S, Murali G. Analytical study of nonlinear behavior and convection patterns in Darcy-Brinkman porous medium with Maxwell-Cattaneo ferro convection. J Mines Met Fuels. 2025; 73(2):437-445. https://doi.org/10.18311/jmmf/2025/47828
15. Murali G, Madhu JV, Deepa G. *et al.* Hall current and MHD impacts on a 3D Maxwell nanofluid flow across a porous stretching surface. Theor Math Phys. 2025; 223:899–914. https://doi.org/10.1134/S0040577925060030
16. Murali G, Madhu JV, Deepa G, Suresh P, Nagaraju B. Three-dimensional oldroyd-B fluid flow past a stretching surface with magnetic field, nanofluid particles and Cattaneo-Christov double diffusion effects. Johns Matthey Technol Rev. 2025; 69(2):299-320. https://doi.org/10.1595/205651325X17375408788409
17. Shah SAA, Ahammad NA, Din EMTE, Gamaoun F, Awan AU, Ali B. Bio-convection effects on Prandtl hybrid nanofluid flow with chemical reaction and motile microorganism over a stretching sheet. Nanomaterials. 2022; 12(13):2174. https://doi.org/10.3390/nano12132174
18. Dharmaiah G, Mebarek-Oudina F, Balamurugan KS, Vedavathi N. Numerical analysis of the magnetic dipole effect on a radiative ferromagnetic liquid flowing over a porous stretched sheet. Fluid Dyn Mater. Process. 2024; 20(2):293-310. https://doi.org/10.32604/fdmp.2023.030325
19. Raza J, Mebarek-Oudina F, Ali H, Sarris IE. Slip effects on Casson nanofluid over a stretching sheet with activation energy: RSM analysis. Frontiers in Heat and Mass Transfer. 2024; 22(4):1017-1041. https://doi.org/10.32604/fhmt.2024.052749
20. Mebarek-Oudina F, Dharmaiah G, Rama Prasad JL, Vaidya H, Kumari MA. Investigation of magnetohydrodynamic Burgers' fluid flow under cylinder stretching: effects of internal heat generation and absorption. Int J Thermophys. 2025; 25:100986. https://doi.org/10.1016/j.ijft.2024.100986
21. Anil Kumar M, Mebarek-Oudina F, Mangathai P, Shah NA, Vijayabhaskar CH, Venkatesh N, Fouad Y. The impact of Soret Dufour and radiation on the laminar flow of a rotating liquid past a porous plate via chemical reaction. Mod Phys Lett B. 2025; 39(10):2450458. https://doi.org/10.1142/S021798492450458X
22. Mohammad Fayz-Al-Asad, Mebarek-Oudinab F, Vaidya H, Hasan MS, Sarker MMA, Ismail AI. Finite element analysis for magneto-convection heat transfer performance in vertical wavy surface enclosure: fin size impact. Front Heat Mass Transf. 2024; 22(3):817-837. https://doi.org/10.32604/fhmt.2024.050814
23. Ramasekhar G, Mebarek-Oudina F, Suneetha S, Vaidya H, Selvi PD. Computational simulation of Casson hybrid nanofluid flow with Rosseland approximation and uneven heat source/sink. Int J Thermofluid. 2024; 24:100893. https://doi.org/10.1016/j.ijft.2024.100893
24. Sivaiah S, Gundagani, Karanamu MP. Analysis of heat and mass transfer effects on an isothermal vertical oscillating plate. WJST. 2012; 9(4):407-415.
25. Khan SA, Imran M, Waqas H, Muhammad T, Yasmin S, Alhushaybari A. Numerical analysis of multiple slip effects on CuO/MgO/TiO2-water ternary hybrid nanofluid with thermal and exponential space-based heat source. Tribology International. 2024; 197:109778. http://dx.doi.org/10.1016/j.triboint.2024.109778
26. Kingston TA, Weibel JA, Garimella SV. Time-resolved characterization of microchannel flow boiling during transient heating: part 1-dynamic response to a single heat flux pulse. Int J Heat Mass Transf. 2020; 154:119643. https://doi.org/10.1016/j.ijheatmasstransfer.2020.119643
27. Firdous H, Husnine SM, Hussain F, Nazeer M. Velocity and thermal slip effects on two-phase flow of MHD Jeffrey fluid with the suspension of tiny metallic particles. Physica Scripta. 2020; 96(2):025803. https://doi.org/10.1088/1402-4896/abcff0
28. Wang CS, Wei, TC, Shen PY, Liou TM. Lattice Boltzmann study of flow pulsation on heat transfer augmentation in a louvered microchannel heat sink. Int J Heat Mass Transf. 2020; 148:119139. https://doi.org/10.1016/j.ijheatmasstransfer.2019.119139

29. Yang Y, Zhou L, Shi W, He Z, Han Y, Xiao Y. Interstage difference of pressure pulsation in a three-stage electrical submersible pump. J Pet Sci Eng.. 2021; 196:107653. https://doi.org/10.1016/j.petrol.2020.107653
30. Ali A, Si Q, Yuan J, Shen C, Cao R, Saad Algarni T, Aslam B. Investigation of energy performance, internal flow, and noise characteristics of a miniature drainage pump under water-air multiphase flow: Design and part load conditions. Int J Environ Sci Technol. 2022; 19(8):7661-7678. https://doi.org/10.1007/s13762-021-03619-1
31. Noh HY, Kim SJ. Numerical simulation of pulsating heat pipes: parametric investigation and thermal optimization. Energy Conv Manag. 2020; 203:112237. https://doi.org/10.1016/j.enconman.2019.112237
32. Markal B, Varol R. Thermal investigation and flow pattern analysis of a closed-loop pulsating heat pipe with binary mixtures. J Braz Soc Mech Sci Eng. 2020;42(10):1-18. https://doi.org/10.1007/s40430-020-02618-6
33. Esfe MH, Bahiraei M, Torabi A, Valadkhani M. A critical review on pulsating flow in conventional fluids and nanofluids: thermo-hydraulic characteristics. Int Commun Heat Mass Transfer. 2021; 120:104859. https://doi.org/10.1016/j.icheatmasstransfer.2020.104859
34. Somasundaram R, Reddy AS. Pulsating flow of electrically conducting couple stress nanofluid in a channel with ohmic dissipation and thermal radiation-Dynamics of blood. Proceedings of the Institution of Mechanical Engineers, Part E: Journal of Process Mechanical Engineering. 2021; 235(6):1895-1909. https://doi.org/10.1177/09544089211025177
35. Cornejo I, Nikrityuk P, Lange C, Hayes RE. Influence of upstream turbulence on the pressure drop inside a monolith. Chem Eng Process: Process Intensif. 2020; 147:107735. https://doi.org/10.1016/j.cep.2019.107735
36. Nikolayev VS. Physical principles and state-of-the-art of modeling of the pulsating heat pipe: A review. Appl Therm Eng. 2021; 195:117111. https://doi.org/10.1016/j.applthermaleng.2021.117111
37. Pagliarini L, Cattani L, Bozzoli F, Mameli M, Filippeschi S, Rainieri S, Marengo M. Thermal characterization of a multi-turn pulsating heat pipe in microgravity conditions: Statistical approach to the local wall-to-fluid heat flux. Int J Heat Mass Transf. 2021; 169:120930. https://doi.org/10.1016/j.ijheatmasstransfer.2021.120930
38. Pavan CA, Guerra-Garcia C. Nanosecond pulsed discharge dynamics during passage of a transient laminar flame. Plasma Sources Sci Technol. 2022. https://doi.org/10.1088/1361-6595/aca0bc
39. Li Q, Wang C, Wang Y, Wang, Z, Li H, Lian C. Study on the effect of the adiabatic section parameters on the performance of pulsating heat pipes. Appl Therm Eng. 2020; 180:115813. https://doi.org/10.1016/j.applthermaleng.2020.115813
40. Lohse D. Fundamental fluid dynamics challenges in inkjet printing. Annu Rev Fluid Mech. 2022; 54:349-382. https://doi.org/10.1146/annurev-fluid-022321-114001
41. Narayan S, Moravec DB, Dallas AJ, Dutcher CS. Droplet shape relaxation in a four-channel microfluidic hydrodynamic trap. Phys Rev Fluids. 2020; 5(11):113603. https://doi.org/10.1103/PhysRevFluids.5.113603
42. Alhajaj Z, Bayomy AM, Saghir MZ, Rahman MM. Flow of nanofluid and hybrid fluid in porous channels: experimental and numerical approach. Int J Thermofluid. 2020; 1:100016. https://doi.org/10.1016/j.ijft.2020.100016
43. Pietrasanta L, Mameli M, Mangini D, Georgoulas A, Michè N, Filippeschi S, Marengo M. Developing flow pattern maps for accelerated two-phase capillary flows. Exp Therm Fluid Sci. 2020; 112:109981. https://doi.org/10.1016/j.expthermflusci.2019.109981
44. Gundagani M, Babu NVN. Effect of radiation on MHD convection flow past a vertical permeable moving plate. IJAAS. 2012; 1(1):19-28. https://doi.org/10.14419/ijamr.v1i2.45
45. Murali G, Lakshmi P, Amarnath M *et al*. Three-dimensional MHD flow of a radiative Eyring–Powell nanofluid: Exploring Hall effects and heat transfer. Theor Math Phys. 2025; 223:1070–1086. https://doi.org/10.1134/S0040577925060170
46. Zhao J, Jian Q, Huang Z. Visualization study on enhancing water transport of proton exchange membrane fuel cells with a dead-ended anode by generating fluctuating flow at the anode compartment. Energy Convers Manag. 2020; 206:112477. https://doi.org/10.1016/j.enconman.2020.112477
47. Tanuku PK, Mamidi LP, Gundagani M. Modelling and analysis of three-dimensional chemically reacting, radiating Casson-nanofluid flow: thermophoresis and Brownian motion effects. Acta Polytechnica. 2024; 64(5):455-463. https://doi.org/10.14311/AP.2024.64.0455
48. Poornakantha T, Laksmiprsanna M, Murali G. Modelling and analysis of three-dimensional Maxwell-nanofluid flow over a bi-directional stretching surface in the presence of a magnetic field. Int J Eng Model. 2025; 38(1):53-72. https://doi.org/10.31534/engmod.2025.1.ri.04d.